PHYSICAL REVIEW E **68**, 056501 (2003)

Phase dependence of relativistic electron dynamics and emission spectra in the superposition of an ultraintense laser field and a strong uniform magnetic field

Xinkui He, B. Shuai, X. C. Ge, R. X. Li,* and Z. Z. Xu
Laboratory for High Intensity Optics, Shanghai Institute of Optics and Fine Mechanics, Chinese Academy of Sciences, Shanghai 201800, People's Republic of China
(Received 13 May 2003; published 21 November 2003)

The phase dependence of the dynamics and emission spectra of a fully relativistic electron in the superposition of an ultraintense plane wave laser field and a strong uniform magnetic field has been investigated. It is found that the effect of changing the initial laser phase is quite different for circularly and linearly polarized laser fields. For circular polarization only the axis of the helical trajectory is changed with variation of the initial laser field phase. However, for linear polarization, the effect of changing the initial phase is opposite in the two parameter regions divided by the resonance condition $r=1$ (r stands for the ratio between the reduced cyclotron frequency and laser frequency). When $r<1$, with increase in the initial laser field phase η_0 from 0 to $\pi/2$, both the radius of the electron's helical trajectory and the height of the peak related to the uniform magnetic field are decreased, and these two physical values are increased with an increase in the laser initial phase when $r>1$. The phase dependence of the electron's energy and velocity components was also studied. Some beat structure is found when $\eta_0=0$ and this structure is absent when $\eta_0=\pi/2$.

DOI: 10.1103/PhysRevE.68.056501 PACS number(s): 52.38.Kd

I. INTRODUCTION

Recent advances in table-top, ultrahigh-intensity lasers have led to significant renewed interest in the classic problems of Thomson and Compton scattering. As the laser intensity increases, various nonlinear phenomena has been found, such as figure-8 orbits [1], nonlinear Thomson scattering [2–5], harmonic generation [4–6], self-focusing of the laser pulse in a plasma channel [7,8], etc. The main motivation to study these phenomena is the prospect of producing table-top particle accelerators and x-ray sources.

Because of the ultrahigh intensity of the laser field and the ultrashort duration of the laser pulse, the phase at which the electron experiences the laser pulse will be important. For instance, electrons created during the ionization of the gas at different phases of the laser pulse have completely different behaviors [9,20,21]. A finite plasma temperature will also lead to a spread in the initial phase. In interacting with curved wave fronts, electrons will experience different initial phases at the same axial position. There is much work concerning electrons interacting with ultraintense lasers, but relatively little work has been reported on the phase dependence of the properties of the interaction. The work of Gunn and Ostriker concerned this problem many years ago [10]. In a more recent paper [11], He *et al.* studied the same problem again. They found that the electron orbit and the Thomson scattering spectra depend critically on the phase in which the electrons experience the laser electric field. The Thomson spectra no longer occur at integer multiples of the laser frequency.

In this work, we study the interaction of an electron with an ultraintense laser field, with an added strong uniform magnetic field parallel to the laser propagation direction. This problem is important for the understanding of laser-plasma interaction and the related problems of high-energy electron emission [12–14], as well as for the interpretation and understanding of current laser-assisted fusion experiments [15]. Recently, Connerade and Keitel investigated this problem with lower laser intensity (10^{16} W/cm^2) [16]. They found that, in addition to the usual odd harmonic, there is an even harmonic in the direction of the laser propagation because of the broken symmetry. In a more recent paper [17], Salamin and Faisal presented an exact analytic solution of the problem. They found that, for observation along the same direction as the laser propagation and the magnetic field, light at the frequency of the laser and another frequency Ω_0 is scattered, and Ω_0 is dependent on the electron initial velocity, the intensity and frequency of the laser, and the strength of the magnetic field. Because Ω_0 would be absent in the absence of the added uniform magnetic field, Salamin and Faisal called it the magnetic peak. The magnetic peak is important because it represents the difference between the current model and classic Thomson scattering.

In this paper, we investigate the phase dependence of the dynamics and emission spectra of a fully relativistic electron in the simultaneous presence of an ultraintense plane wave laser field and a strong uniform magnetic field for the first time to the best of our knowledge. The results show that the effect of changing the initial laser phase is quite different for the cases of circularly and linearly polarized laser fields. For circular polarization only the axis of the helical trajectory is changed with variation of the initial laser field phase. However, for linear polarization, the effect of changing the initial phase is different in the two parameter regions divided by $r=1$, where r stands for the frequency ratio

$$r=\frac{\omega_c}{\omega_l}\sqrt{(1+\beta_0)/(1-\beta_0)},\qquad(1)$$

Where $\beta_0=v_0/c$ is the initial electron speed normalized by

*Electronic address: ruxinli@mail.shcnc.ac.cn

c, $\omega_c = eB_s/mc$ is the cyclotron frequency of the electron moving in the magnetic field B_s, and ω_l is the frequency of the laser field. When $r=1$, the electron can gain maximum energy from the laser field, so $r=1$ is called the resonance condition [19]. Our results also indicate that the magnetic peak (the peak related to the uniform magnetic field) is decided by the helical trajectory of the electron's movement.

The rest of the paper is organized as follows. In Sec. II we formulate the problem. In Sec. III, the numerical results for the electron trajectories, velocity components, and energy for different initial laser field phases are given graphically. In Sec. IV the emission spectra calculated numerically on the basis of the general light-emission cross section expression are presented and discussed for different initial laser field phases. Finally, a summary of our results and conclusions is given in Sec. V.

II. FORMULATION

We consider a relativistic electron with mass m and charge $-e$, in the simultaneous presence of an intense plane wave laser field and a strong uniform magnetic field. The vector potential of the fields can be represented by

$$\mathbf{A} = A_l[\hat{\mathbf{i}}\delta\cos\eta + \hat{\mathbf{j}}\sqrt{1-\delta^2}\sin\eta] - \frac{B_s}{2}(\hat{\mathbf{i}}y - \hat{\mathbf{j}}x). \quad (2)$$

The first term in Eq. (2) represents a plane wave of arbitrary polarization with field strength A_l, where $\eta = \omega_l t - \mathbf{k}\cdot\mathbf{r} + \eta_0$ is the phase of the laser field with frequency ω_l, η_0 is the initial laser field phase at $t=0$, and $\mathbf{k}$ is the wave vector of the laser field, pointing in the positive z direction. δ gives the degree of ellipticity; $\delta=1$ for linear polarization and $1/\sqrt{2}$ for circular polarization. The second term represents the uniform magnetic field in the same (z) direction. The electric and magnetic fields can be derived from the equations

$$\mathbf{E} = -\frac{1}{c}\frac{\partial\mathbf{A}}{\partial t}, \quad \mathbf{B} = \boldsymbol{\nabla}\times\mathbf{A}. \quad (3)$$

The behavior of the electron in the superposed fields is governed by the relativistic Lorentz equation

$$\frac{d\mathbf{P}}{dt} = -e(\mathbf{E} + \boldsymbol{\beta}\times\mathbf{B}), \quad (4)$$

and the energy equation

$$\frac{d\epsilon}{dt} = -ec\boldsymbol{\beta}\cdot\mathbf{E}, \quad (5)$$

where $\epsilon = \gamma mc^2$, $\mathbf{P} = \gamma mc\boldsymbol{\beta}$, $\boldsymbol{\beta}$ is the electron velocity normalized by c, the speed of light, and $\gamma = (1-\beta^2)^{-1/2}$.

From Eqs. (4) and (5) we can derive the component form of the motion equation [17],

$$\frac{d(\gamma\beta_x)}{dt} = -q\delta\omega_l(1-\beta_z)\sin\eta - \omega_c\beta_y, \quad (6)$$

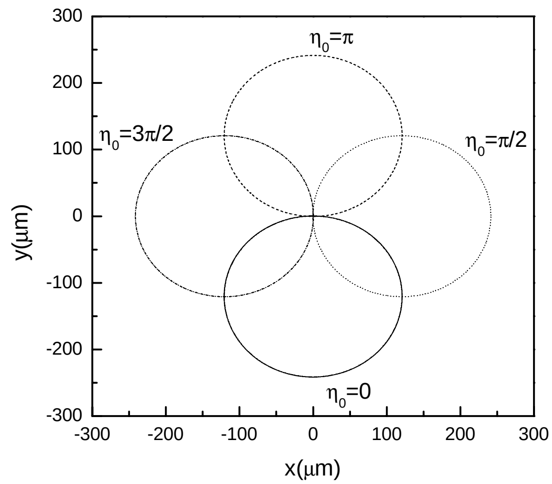

FIG. 1. Projection of the electron trajectory for different initial laser field phases η_0 on the xy plane for circular polarization. The trajectory is plotted over 450 field cycles and the electron is initially at rest. $q=3$, $\lambda=0.8$ μm, and the strength of the uniform magnetic field $B_s=30$ T.

$$\frac{d(\gamma\beta_y)}{dt} = q\sqrt{1-\delta^2}\omega_l(1-\beta_z)\cos\eta + \omega_c\beta_x, \quad (7)$$

$$\frac{d(\gamma\beta_z)}{dt} = q\omega_l[\sqrt{1-\delta^2}\beta_y\cos\eta - \delta\beta_x\sin\eta], \quad (8)$$

$$\frac{d\gamma}{dt} = q\omega_l[\sqrt{1-\delta^2}\beta_y\cos\eta - \delta\beta_x\sin\eta], \quad (9)$$

where $q = eA_l/mc^2$ is the dimensionless intensity parameter of the laser field.

III. PHASE DEPENDENCE OF THE ELECTRON'S DYNAMICS

A. Trajectory

Following Salamin and Faisal's analysis procedure [17], we can derive the trajectory equation of the electron in the superposition of the laser field and the uniform magnetic field with arbitrary initial laser field phase,

$$x(\eta) = \frac{cqr}{\omega_c}\left[\frac{\delta + r\sqrt{1-\delta^2}}{1-r^2}\sin\eta + \frac{\sqrt{1-\delta^2}}{r}\sin\eta_0\right] + a\cos(r\eta) - b\sin(r\eta), \quad (10)$$

$$y(\eta) = -\frac{cqr}{\omega_c}\left[\frac{r\delta + \sqrt{1-\delta^2}}{1-r^2}\cos\eta + \frac{\delta}{r}\cos\eta_0\right] + a\sin(r\eta) + b\cos(r\eta), \quad (11)$$

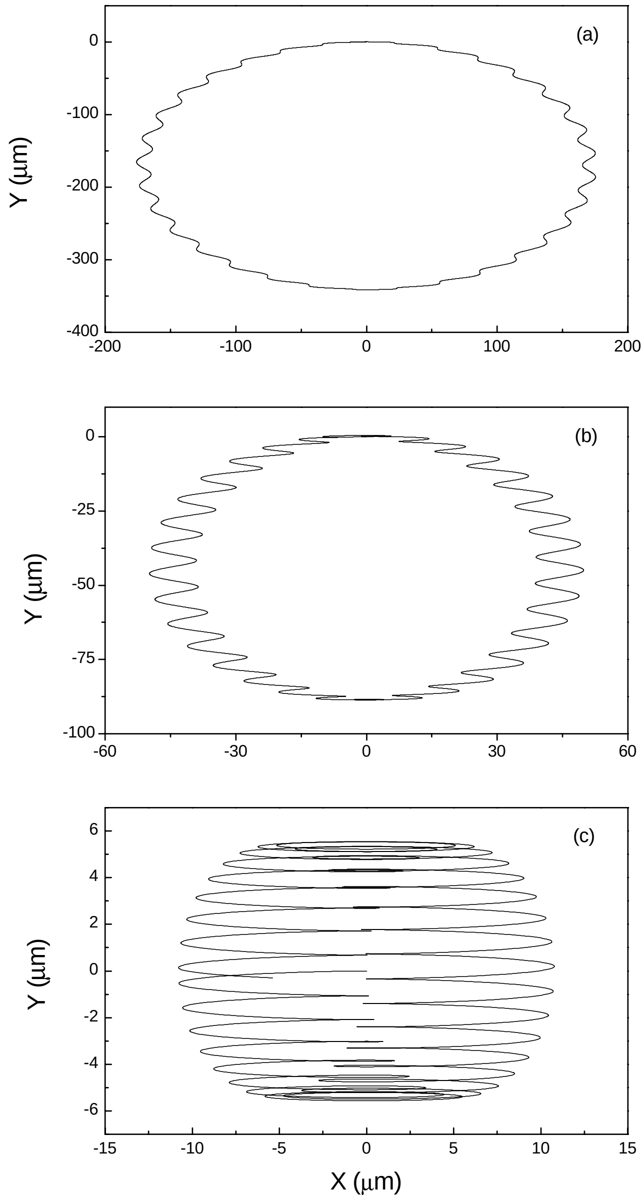

FIG. 2. Projection of the electron trajectory on the *xy* plane for linear polarization when $r=0.0316$. The trajectory is plotted over 32 field cycles, with initial speed $\beta_0=0.99$. The parameters of the laser field and uniform magnetic field are the same as in Fig. 1. $\eta_0=$(a) 0, (b) $\pi/2.4$, (c) $\pi/2$.

$$z(\eta)=\frac{c}{2\omega_l}\frac{1+\beta_0}{1-\beta_0}\left\{\left(\xi_0+\frac{2\beta_0}{1+\beta_0}\right)(\eta-\eta_0)\right.$$
$$+\xi_1[\sin(2\eta)-\sin(2\eta_0)]$$
$$+\xi_2\{\cos[(1+r)\eta]-\cos[(1+r)\eta_0]\}$$
$$-\xi_3\{\cos[(1-r)\eta]-\cos[(1-r)\eta_0]\}$$
$$-\xi_4\{\sin[(1+r)\eta]-\sin[(1+r)\eta_0]\}$$
$$\left.-\xi_5\{\sin[(1-r)\eta]-\sin[(1-r)\eta_0]\}\right\}, \quad (12)$$

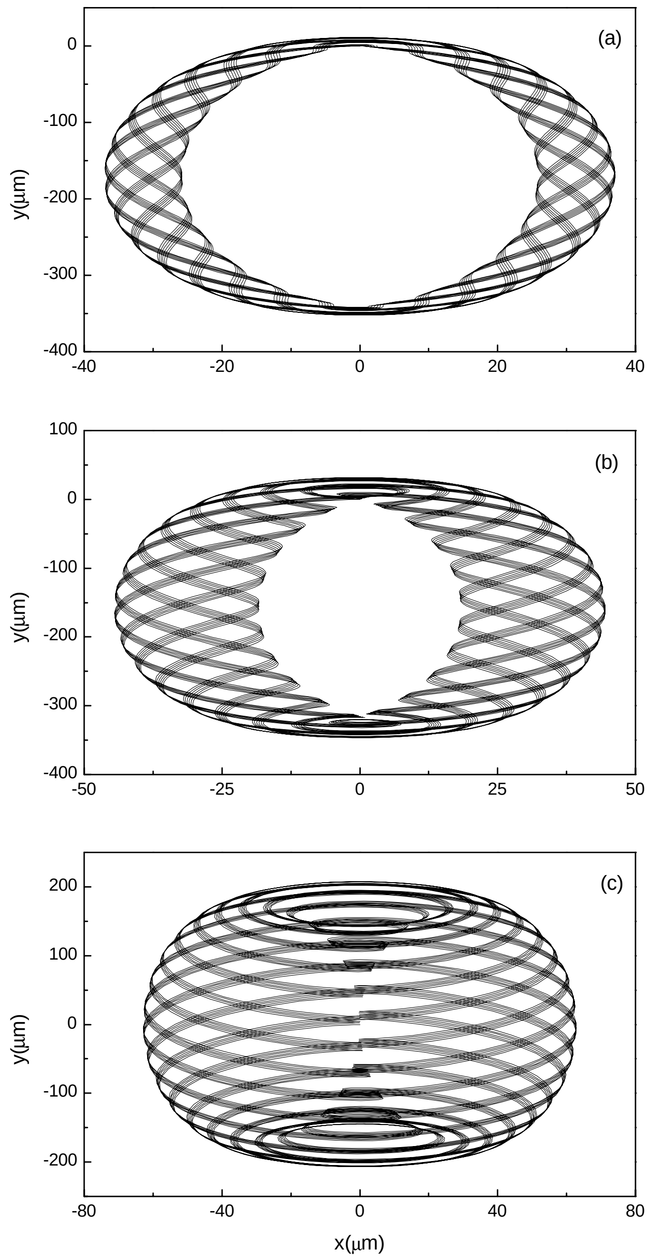

FIG. 3. Same as Fig. 2, but for $r=1.4173$, with $\gamma_0=100$ or $\beta_0=0.999\,995$. $\eta_0=$(a) 0, (b) $\pi/8$, (c) $\pi/2$.

$$\gamma=\gamma_0+\frac{\gamma_0}{2}(1+\beta_0)\{\xi_0+2\xi_1\cos(2\eta)-\xi_2(1+r)$$
$$\times\sin[(1+r)\eta]+\xi_3(1-r)\sin[(1-r)\eta]$$
$$-\xi_4(1+r)\cos[(1+r)\eta]$$
$$-\xi_5(1-r)\cos[(1-r)\eta]\}, \quad (13)$$

where

$$\xi_0=\frac{q^2(1+r^2+4r\delta\sqrt{1-\delta^2})}{2(1-r^2)^2}+\left(\frac{\omega_c}{c}\right)^2(a^2+b^2),$$

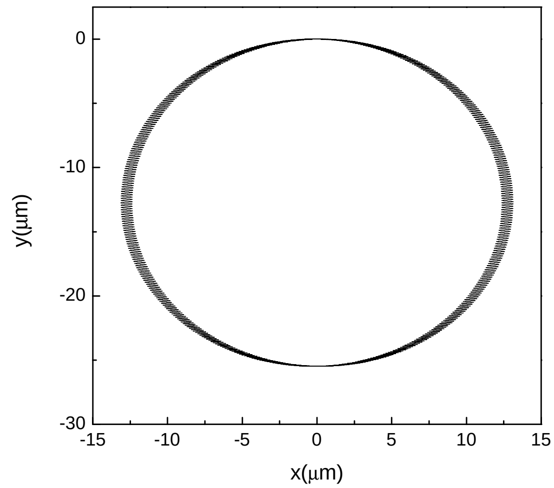

FIG. 4. Projection of the electron trajectory on the *xy* plane for linear polarization when $\beta_0=0$. The trajectory is plotted over 450 field cycles. $\eta_0=\pi/2.1$. The parameters of the laser field and uniform magnetic field are the same as in Fig. 1.

$$\xi_1=\frac{q^2(2\delta^2-1)}{4(1-r^2)},$$

$$\xi_2=\frac{\omega_c}{c}\frac{qa(\delta-\sqrt{1-\delta^2})}{(1+r)^2},\quad \xi_3=\frac{\omega_c}{c}\frac{qa(\delta+\sqrt{1-\delta^2})}{(1-r)^2},$$

$$\xi_4=\frac{\omega_c}{c}\frac{qb(\delta-\sqrt{1-\delta^2})}{(1+r)^2},\quad \xi_5=\frac{\omega_c}{c}\frac{qb(\delta+\sqrt{1-\delta^2})}{(1-r)^2},$$

$$a=\frac{cq}{\omega_c(1-r^2)}[(\delta+r\sqrt{1-\delta^2})\cos(\eta_0)\sin(r\eta_0)-(\sqrt{1-\delta^2}+r\delta)\sin(\eta_0)\cos(r\eta_0)], \tag{14}$$

$$b=\frac{cq}{\omega_c(1-r^2)}[(\delta+r\sqrt{1-\delta^2})\cos(\eta_0)\cos(r\eta_0)+(\sqrt{1-\delta^2}+r\delta)\sin(\eta_0)\sin(r\eta_0)]. \tag{15}$$

From Eqs. (14) and (15) we know that a and b are constants decided by the initial phase and the polarization of the

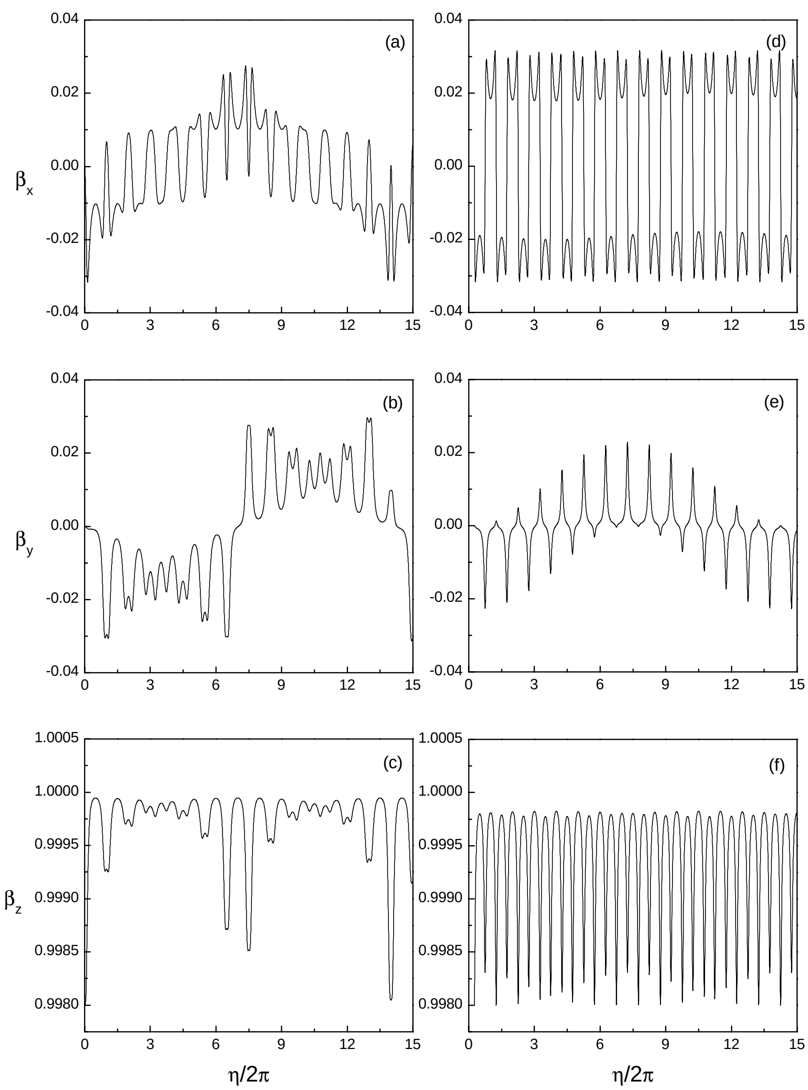

FIG. 5. Components of the scaled velocity vector of the electron are shown over 15 field cycles. The initial speed of the electron is $0.998c$. The parameters of the laser field and uniform magnetic field are the same as in Fig. 1. $\eta_0=$(a)–(c) 0, (d)–(f) $\pi/2$.

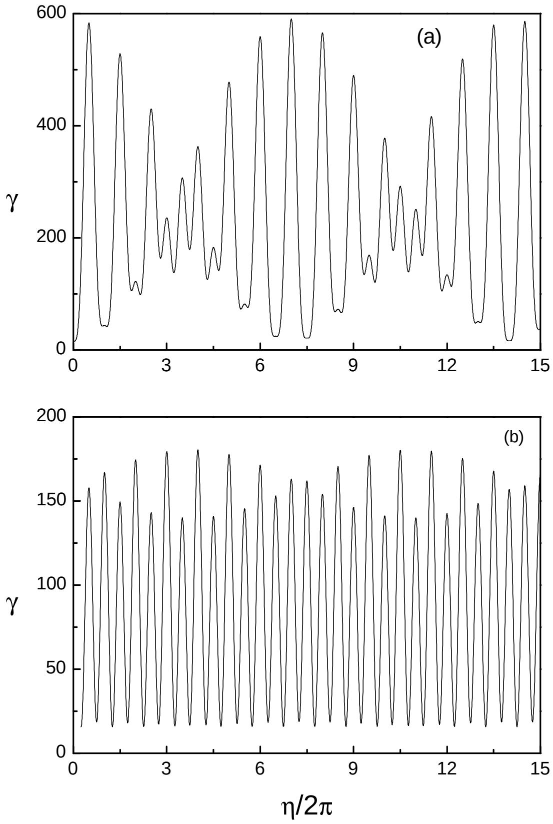

FIG. 6. Scaled electron energy whose velocity components are given in Fig. 5. $\eta_0 =$(a) 0, (b) $\pi/2$.

laser field. If $\eta_0 = 0$, then the constant a will be 0, and only the constant b remains. This is the case described in [17]

In the case of circular polarization (ellipticity parameter $\delta = 1/\sqrt{2}$), for different initial laser phases, we show the trajectory of the electron in Fig. 1. We learned from Salamin and Faisal's work [17] that the electron will follow a wiggly helical path whose axis is parallel to common direction of $\mathbf{B}_s$ and $\mathbf{k}$ regardless of polarization, so in Fig. 1 we just present the projection of the trajectory on the plane perpendicular to the laser propagation. We can see that for different initial laser phases the axis of the helical trajectory is different. So if there are many electrons, and they enter into the superposition field at different times, the diameter of the cross section of the electrons will be twice that of the helical trajectory; this is a disadvantage to the acceleration of electrons using this model. This result is not hard to understand. The direction of the electric field of a circularly polarized wave varies with the phase of the laser, so when the electron comes into the laser field it will gain different transverse velocity components $\mathbf{v}_{0t}$ in the electric field direction. However, from this moment, the electron starts to experience the bending effects of $\mathbf{B}_s$, and the bending is in the direction of $-(e/c)\mathbf{v}_{0t}\times\mathbf{B}_s$. So with different initial laser phases there will be different directions of $\mathbf{v}_{0t}$ and different bending directions, and thus a different helical axis. From this discussion we can also conclude that the other physical characteristics will not change with the initial laser field phase for the case of circular polarization, so we just discuss the linear polarization case in the remainder of this paper.

In the case of linear polarization, when $r<1$, the projection of the trajectory on the xy plane is shown in Fig. 2. One can see that, when the initial laser phase changes from 0 to $\pi/2$, the radius of the helical trajectory is decreased, with a minimum value at $\pi/2$. Note that the amplitude of the wiggles does not change, so it seems that the wiggles become larger. When $r>1$, the same orbital projection is presented in Fig. 3. It shows that the radius of the helical trajectory is increased with increase of the laser field phase from 0 to $\pi/2$, and the amplitude of the wiggles is increased too. We found that in the linear polarization case the helical axis also changes with the initial laser phase.

In Salamin and Faisal's recent paper [17], the wiggles appeared to be controlled by the initial electron speed β_0 and were absent when $\beta_0 = 0$. We found that the wiggles also exist under this condition as shown in Fig. 4. For zero initial laser field phase (the case described in [17]), the amplitude of the wiggles is too small to be found compared with the helical radius, but the wiggles are obvious when $\eta_0 = \pi/2.1$ because of the decrease of the helical radius. We think the wiggles are produced by the combination of the electric and magnetic forces $-(e/c)\boldsymbol{\beta}_0\times\mathbf{B}_l$, which varies periodically.

B. Velocity components and energy

We investigate the phase dependence of the velocity components and energy of the relativistic electron in this subsection. From Eqs. (6)–(9) we can also derive the expressions for the normalized components of the velocity β_x, β_y, β_z:

$$\beta_x = \frac{q(\delta + r\sqrt{1-\delta^2})}{\gamma(1-r^2)}\cos(\eta) - \frac{\omega_c}{\gamma c}[a\sin(r\eta) + b\cos(r\eta)], \tag{16}$$

$$\beta_y = \frac{q(\sqrt{1-\delta^2} + r\delta)}{\gamma(1-r^2)}\sin(\eta) + \frac{\omega_c}{\gamma c}[a\cos(r\eta) - b\sin(r\eta)], \tag{17}$$

$$\beta_z = 1 - \frac{\gamma_0}{\gamma}(1-\beta_0). \tag{18}$$

In Fig. 5 we show the velocity components β_x, β_y, β_z as functions of the laser phase for initial laser field phases 0 and $\pi/2$. Figure 6 shows the energy as a function of the laser phase with the same parameters. The figures clearly show that β_x, β_y, and γ exhibit beat structures at $\eta_0 = 0$, and β_z also exhibits some periodic structure, but all these structures are absent when $\eta_0 = \pi/2$; instead, the curves exhibit oscillation at almost a uniform amplitude (except for β_y). We also found that the maximum value of β_z and the average value of γ are obviously smaller at $\eta_0 = \pi/2$ than that at $\eta_0 = 0$. It seems that the electron exchanges less energy with the laser field when the initial laser field phase is $\pi/2$ than it does when $\eta_0 = 0$.

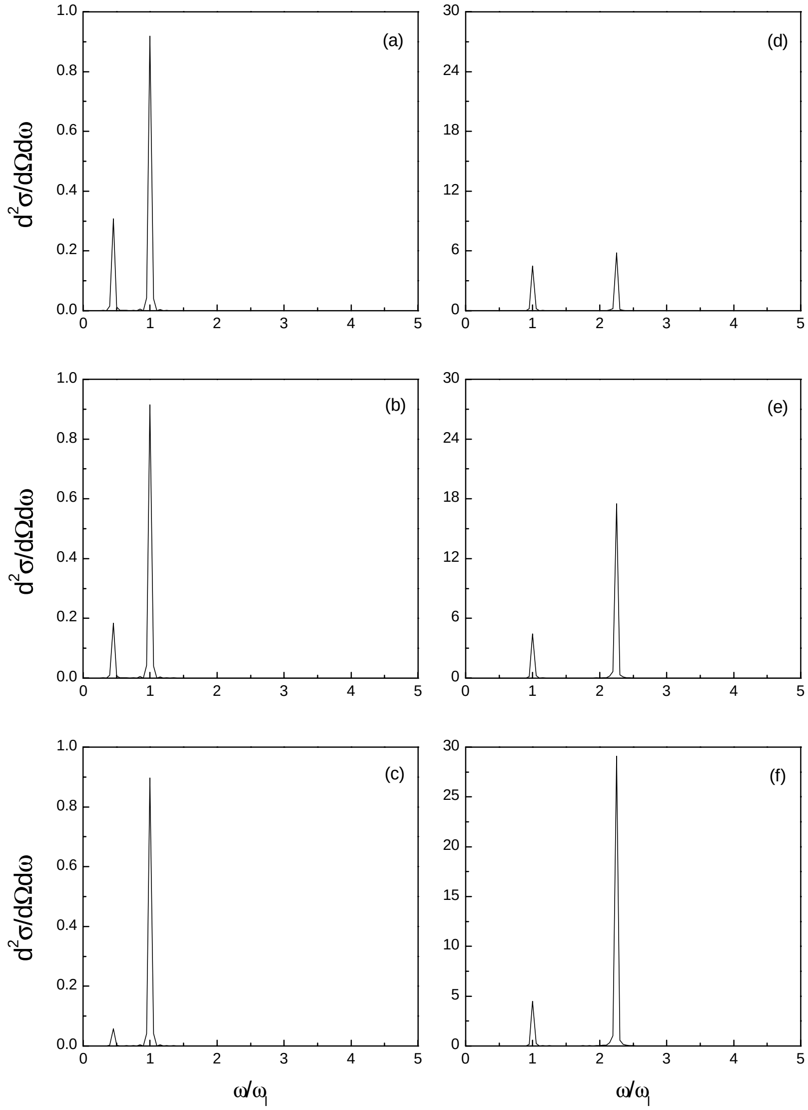

FIG. 7. Spectrum versus normalized frequency ω/ω_l for observation along the laser propagation direction. The numerical integrations were carried out over 30 field cycles with $q=1$, $\lambda=0.8\ \mu$m, $B_s=30$ T. (a)–(c) $r=0.4482$ and $\gamma_0=100$; (d)–(f) $r=2.2409$ and $\gamma_0=500$. (d) $\eta_0=$(a),(d) 0; (b),(e) $\pi/4$; (c),(f) $\pi/2$.

IV. RADIATION SPECTRA

The starting point for calculating the angular and frequency distributions of the radiation is the radiation energy emitted per unit solid angle $d\Omega$ and per unit frequency interval $d\omega$ [18],

$$\frac{d^2E(\omega,\Omega)}{d\Omega\,d\omega}=\frac{e^2}{4\pi^2c}\left|\int_0^T\frac{\mathbf{n}\times[[\mathbf{n}-\boldsymbol{\beta}(t)]\times\dot{\boldsymbol{\beta}}(t)]}{[1-\mathbf{n}\cdot\boldsymbol{\beta}(t)]^2}\times\exp\left\{i\omega\left[t-\frac{\mathbf{n}\cdot\mathbf{r}(t)}{c}\right]\right\}dt\right|^2$$
$$=\frac{e^2}{4\pi^2c}\left|\left[\frac{\mathbf{n}\times\mathbf{n}\times\boldsymbol{\beta}(t)}{1-\mathbf{n}\cdot\boldsymbol{\beta}(t)}\exp\left\{i\omega\left[t-\frac{\mathbf{n}\cdot\mathbf{r}(t)}{c}\right]\right\}\right]\right|_0^T-i\omega\int_0^T\mathbf{n}\times\mathbf{n}\times\boldsymbol{\beta}(t)\exp\left\{i\omega\left[t-\frac{\mathbf{n}\cdot\mathbf{r}(t)}{c}\right]\right\}dt\right|^2. \tag{19}$$

where E denotes the radiated energy, $\mathbf{n}$ is the unit vector in the direction of propagation of the emitted radiation, and T is the time interval over which the incident field is nonzero.

In this work the harmonic generation spectrum is calculated by using the doubly differential cross section [17], given by

$$\frac{d^2\sigma(\omega,\Omega)}{d\Omega\,d\omega}=\frac{1}{T}\frac{8\pi c r_0^2}{(eq\omega_l)^2}\frac{d^2E(\omega,\Omega)}{d\Omega\,d\omega}, \tag{20}$$

where r_0 is the classical electron radius. The spectrum that would be observed along the laser propagation direction is shown in Fig. 7. Consistent with Salamin and Faisal's work, there are only two peaks in the spectrum, the Thomson peak and the magnetic peak. When $r<1$, from Figs. 7(a)–7(c), we can see that the height of the magnetic peak decreases with increase of the laser field initial phase from 0 to $\pi/2$. The contrary result is found in Figs. 7(d)–7(f) when $r>1$. This also indicates that the magnetic peak is decided by the helical trajectory of the electron's movement.

In Fig. 8, we show the radiation spectrum that would be observed along the direction of the laser electric field. We

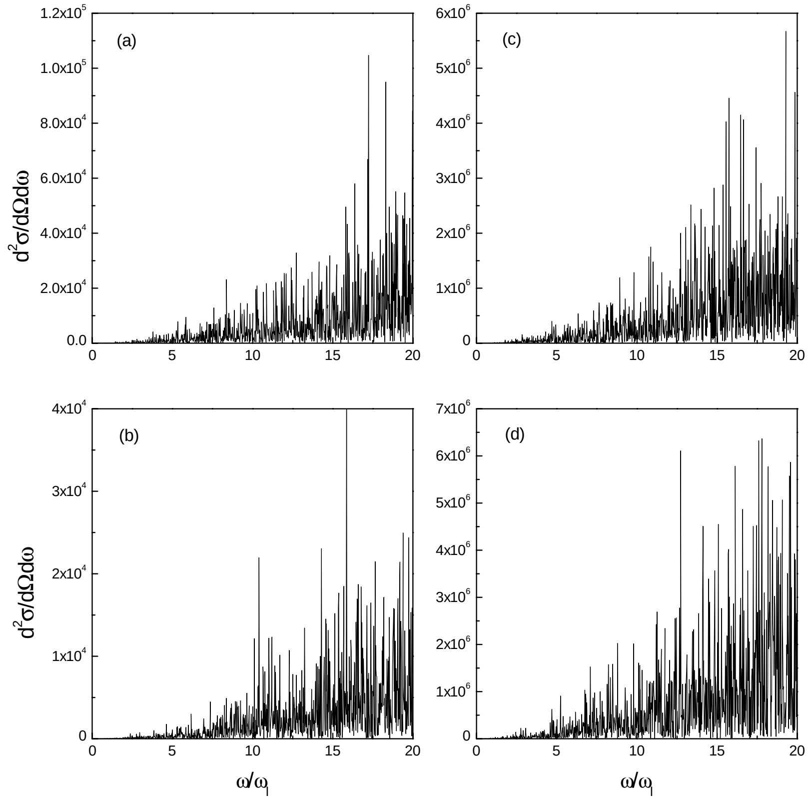

FIG. 8. Same as Fig. 7, but for observation along the electric component of the laser field. (a),(b) $r = 0.4482$ and $\gamma_0 = 100$; (c),(d) $r = 2.2409$ and $\gamma_0 = 500$; (c) $\eta_0 =$ (a),(c) 0; (b),(d) $\pi/2$.

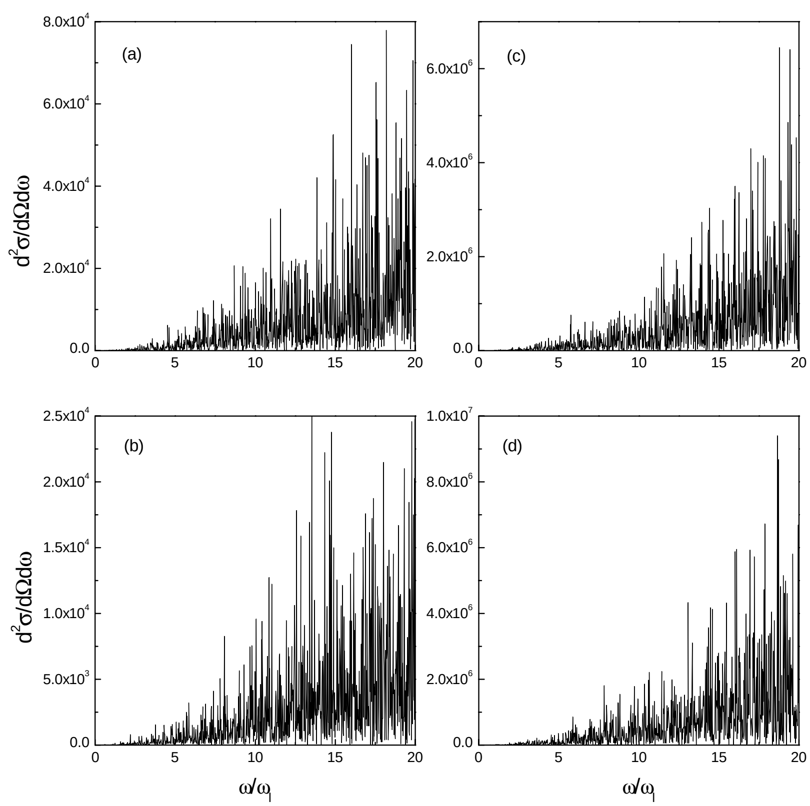

FIG. 9. Same as Fig. 8, but for observation along the magnetic component of the laser field.

also find that the peak heights decrease when η_0 is increased from 0 to $\pi/2$ for $r<1$, and the heights increase for $r>1$. The same result can be found when we observe along the direction of the laser magnetic field (Fig. 9).

V. SUMMARY

We have investigated the phase dependence of the dynamics and emission spectra of a fully relativistic electron in the superposition of an ultraintense plane wave laser field and a strong uniform magnetic field. We have shown that the effect of changing the initial laser phase is quite different for the cases of circularly and linearly polarized laser fields. For circular polarization only the axis of the helical trajectory is changed with variation of the initial laser field phase. However, for linear polarization, the effect of changing the initial phase is different in the two parameter regions divided by the resonance condition $r=1$. When $r<1$, with increase in η_0 from 0 to $\pi/2$, both the radius of the electron's helical trajectory and the height of the magnetic peak are decreased, and these two physical values are increased when $r>1$. The results indicate that the magnetic peak is decided by the helical trajectory of the electron's movement. We also studied the phase dependence of the electron's energy and velocity components and found that they show some beat structure when $\eta_0=0$ and this structure is absent when $\eta_0=\pi/2$. From all these phenomena, we may conclude that, for $r<1$, the energy exchange between the laser field and the relativistic electron is decreased when the initial laser field phase changes from 0 to $\pi/2$, and the result is the contrary when $r>1$.

ACKNOWLEDGMENTS

This work is supported by the Chinese National Natural Science Foundation (Grants No. 19974058 and No. 69925513), the National Key Basic Research Program (Grant No. G1999075200), and the Chinese Academy of Sciences (Grant No. KGCX2-SW-105).

[1] D. Umstadter and T. Norris, IEEE J. Quantum Electron. **33**, 1878 (1997).
[2] E. S. Sarachic and G. T. Schappert, Phys. Rev. D **1**, 2738 (1970).
[3] E. Esarey, S. K. Ride, and P. Sprangle, Phys. Rev. E **48**, 3003 (1993).
[4] S.-Y. Chen, A. Maksimchuk, and D. Umstadter, Nature (London) **396**, 653 (1998).
[5] S.-Y. Chen, A. Maksimchuk, E. Esarey, and D. Umstadter, Phys. Rev. Lett. **76**, 3116 (1996).
[6] S. Baerjee, A. R. Valenzuela, R. C. Shah, A. Masksimchuk, and D. Umstadter, Phys. Plasmas **9**, 2393 (2002).
[7] A. B. Brisov *et al.*, Phys. Rev. Lett. **68**, 2309 (1992).
[8] R. Wagner, S.-Y. Chen, A. Maksimchuk, and D. Umstadter, Phys. Rev. Lett. **78**, 3125 (1997).
[9] Zhinan Zeng, Ruxin Li, Wei Yu, and Zhizhan Xu, Phys. Rev. A **67**, 013815 (2003).
[10] J. E. Gunn and J. P. Ostriker, Astrophys. J. **165**, 523 (1971).
[11] F. He, Y. Y. Lau, Donald P. Umstadter, and Treor Strickler, Phys. Plasmas **9**, 4325 (2002).
[12] B. W. Boreham and H. Hora, Phys. Rev. Lett. **42**, 776 (1979).
[13] L. Cicchitelli, H. Hora, and R. Postle, Phys. Rev. A **41**, 3727 (1990).
[14] H. Hora, *Physics of Laser-Driven Plasmas* (Wiley, New York, 1981).
[15] S. Nakai, Laser Part. Beams **7**, 475 (1989); K. Mima, H. Tahabe, and S. Nakai, *ibid.* **7**, 249 (1989).
[16] J.-P. Connerade and C. H. Keitel, Phys. Rev. A **53**, 2748 (1996).
[17] Y. I. Salamin and F. H. M. Faisal, Phys. Rev. A **58**, 3221 (1998).
[18] J. D. Jackson, *Classical Electrodynamics* (Wiley, New York, 1976).
[19] Y. I. Salamin and F. H. M. Faisal, Phys. Rev. A **62**, 053809 (2000).
[20] P. B. Corkum, Phys. Rev. Lett. **71**, 1994 (1993).
[21] A. de Bohan *et al.*, Phys. Rev. Lett. **81**, 1837 (1998).